INSTITUTE OF PHYSICS PUBLISHING NANOTECHNOLOGY
Nanotechnology **16** (2005) 1172–1176 doi:10.1088/0957-4484/16/8/032

Sub-10 nanometre fabrication: molecular templating, electron-beam sculpting and crystallization of metallic nanowires

M Remeika and A Bezryadin

Department of Physics, University of Illinois at Urbana-Champaign, Urbana, IL 61801, USA

E-mail: bezryadi@uiuc.edu

Received 5 March 2005, in final form 20 April 2005
Published 17 May 2005
Online at stacks.iop.org/Nano/16/1172

Abstract
Homogeneous metallic nanowires with diameters below 10 nm are produced by sputter coating suspended DNA molecules and/or carbon nanotubes. A fabrication method is described that allows 'e-beam nanosculpting', i.e. local modification of the shape of nanowires, with a resolution of ∼3 nm. The process is performed with a focused electron beam (e-beam) in a transmission electron microscope, under direct visual control. We also demonstrate that e-beam radiation can induce local crystallization of nanowires. This method could be used to fabricate novel electronic devices, e.g. single-electron tunnelling transistors, with dimensions below 10 nm, possibly operating at room temperature.

1. Introduction

Regardless of the impressive breakthroughs nanotechnology showed within recent years, fabrication of electronic devices with dimensions below 10 nm remains very challenging. For example, a typical resolution of electron-beam lithography (EBL) is limited to ∼20 nm, although in some most advanced cases the fabrication of short wires as thin as 3 nm [1] has been reported. Thus, new fabrication routes with a resolution comparable with, or better than, 10 nm are very desirable. This is motivated, among other things, by the expectation that certain important types of electronic nanodevices can only be operational at room temperature if their dimensions are reduced to a scale of ∼5 nm or less. Such a requirement occurs because the relevant internal energy scale must be much larger than the energy of thermal fluctuations. For example, in single-electron tunnelling transistors [2, 3], the relevant energy scale is the Coulomb charging energy, $E_c = e^2/2C = e^2/4\pi\varepsilon_0 D$. Here C is the total electric capacitance of the active element of the device (the so-called Coulomb island), which is assumed to be spherical, D is the diameter of the Coulomb island, ε_0 is the permittivity of free space. The condition for the room temperature operation can be written as $E_c \gg E_{th} = k_B T = 4 \times 10^{-21}$ J (here $T = 293$ K is the 'room temperature'). This requirement translates into a size restriction $D < 5.8$ nm (assuming the condition $E_c = 10E_{th}$). It is clear that to meet such requirements some new powerful nanofabrication tools have to be developed, with an ability to produce metallic structures with dimensions well below 10 nm.

Here we describe a novel nanofabrication method that allows us to fabricate nanostructures with dimensions as small as ∼3 nm. This approach consists of two main steps: (i) fabrication of metallic nanowires with diameters of about 10 nm or less, using molecular templates; and (ii) application of a focused electron beam for modification of morphology and local geometrical characteristics of nanowires, with a few-nanometre spatial resolution. It is expected that room temperature charging effects will be observable in electronic transport in such small devices. Below we describe in detail each of these steps and present examples of resulting structures.

Sub-10 nm wide homogeneous metallic nanowires can be fabricated using molecular templates [4]. In this approach a single thread-like molecule, such as a carbon nanotube or a DNA double helix, is placed over a substrate with a narrow (∼0.1–1 μm) trench and a thin layer of metal is deposited over the molecule by sputtering. Examples of such wires are shown in figure 1. These samples were produced as follows. (1) a substrate containing narrow (∼100 nm wide) and long (∼5 mm) trenches (see [4, 5] for details of substrate fabrication) was placed into a solution with λ-DNA molecules and subsequently dried and coated with a desired metal. It is observed that some DNA molecules cross the trench. Such molecules are always stretched by the van der Waals force and produce perfectly straight nanowires. The choice of the

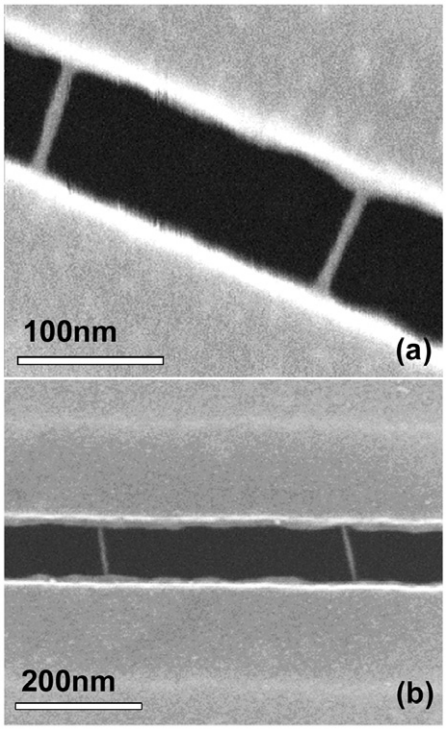

Figure 1. DNA-templated nanowires. The fabrication is done as follows. First a deep trench (∼100 nm wide) is etched into a $SiN/SiO_2/Si$ substrate, as described in [4]. The trench appears black on the SEM micrographs. Double-stranded λ-DNA molecules are deposited onto SiN substrates from a dilute solution and then dried in a nitrogen gas flow. The DNA appears to stretch itself across the trench. Such a suspended and stretched molecule forms an ideal substrate for metallic nanowires. (a) Two DNA-templated metallic nanowires are shown in this SEM micrograph. The molecules are covered with a 4 nm layer of amorphous Os metal (see footnote 1). The widths of the nanowires are ∼8 and ∼11 nm. The nanowires appear homogeneous, i.e. do not show any visible granularity. (b) A pair of DNA-templated nanowires, coated with 4 nm MoGe amorphous alloy. The wires, which also appear homogeneous, measure about 7 nm in width and ∼85 nm in length.

coating metal is important. We observed that Au or AuPd coatings produce visible non-homogeneity (granularity) in the wires (figure 2). This is because these metals are not truly amorphous. In principle the adhesion of such metals to the underlying molecules can be improved by sputtering a Ti sticking layer [6]. Here we follow the approach of [4] and use amorphous metals to coat the molecules and thus obtain highly homogeneous nanowires with diameters below 10 nm, shown in figure 1. The first micrograph (figure 1(a)) presents a pair of wires produced by Os metal coating of suspended DNA molecules[1]. The wires measure about 8 and 11 nm in width. No granularity is visible. Another suitable material is the $Mo_{79}Ge_{21}$ alloy. It gives homogeneous superconducting wires, which can be produced on nanotube templates [4], as well as on DNA templates [7]. Such DNA-templated wires exhibit metallic behaviour and superconductivity at low temperatures [7], confirming their homogeneity. Note that in previous attempts at metallizing DNA molecules it proved very challenging to form thin homogeneous wires [8, 9]. In

[1] OPC-60A, Osmium Plasma Coater. Manufactured by Laser Techno Co. Ltd. Distributed by Scanning Probe Inc. (SPI).

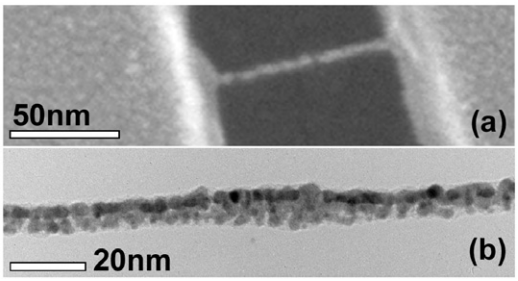

Figure 2. DNA-templated AuPd nanowire. The fabrication is similar to that for the figure 1 examples. (a) shows λ-DNA placed across a ∼100 nm wide trench, then dried and subsequently sputter coated with a 1.5 nm thick layer of AuPd. This alloy is not truly amorphous. Therefore a significant granularity in the wire is clearly visible on the SEM micrograph presented. Some granularity patterns are also visible in thin AuPd film around the trench. The width of the wire is ∼6 nm. (b) A TEM micrograph of an equivalently prepared wire. The granularity is more pronounced in this image.

experiments with carbon nanotube templates it was found that nanowires with a high degree of homogeneity can be also formed by sputter deposition of metallic Nb on carbon nanotubes [10][2]. In the experiments on electron-beam induced crystallization and sculpting (described below) we used carbon-nanotube-templated Nb or MoGe wires.

We demonstrate the possibility of modifying the crystal structure and geometric parameters of nanowires, with a high spatial resolution of approximately 3 nm. A high energy focused electron beam is used for this purpose, under direct visual control in a transmission electron microscope (TEM).

2. Experimental methods

Samples used for e-beam sculpting were prepared by dipping a TEM holey carbon grid in an isopropyl alcohol solution containing fluorinated carbon nanotubes[3]. Consequently the grids were dried with nitrogen gas and sputter coated with a 3–6 nm film of Nb or $Mo_{21}Ge_{79}$. Magnetron DC sputtering of Nb was done at 2 mTorr Ar gas pressure, using a vacuum chamber with base pressure 10^{-7} Torr, equipped with a liquid nitrogen trap. The same method was previously applied for making Nb superconducting nanowires, used in a study of phase slip effects [10] (see footnote 2). The MoGe alloy was sputtered in the same sputtering system, with 4 mTorr of Ar gas. Resulting wires ranged from 5 to 10 nm in width.

Electron irradiation was performed in a 200 keV JEOL JEM-2010F transmission electron microscope, equipped with a field emission gun (FEG). The intensity of the beam was adjusted by varying condenser apertures and spot sizes as well as focusing and spreading the beam. The current density was approximated by dividing the total electron current by the area covered by the beam. This approximation yielded results consistent within ∼20% between different experiments, which is quite sufficient since the results are controlled by direct imaging in the same TEM machine and can be adjusted if necessary.

[2] The Nb wires studied in this work were most probably amorphous. The crystal structure may have been generated during imaging in TEM. All measurements were performed before the TEM imaging.

[3] Carbon nanotubes purchased from Carbon Nanotechnologies Inc.

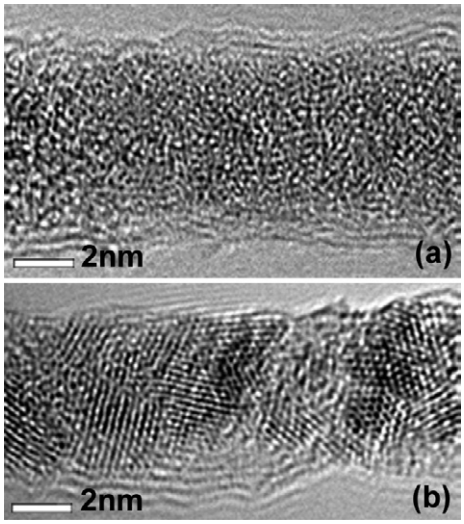

Figure 3. Electron-beam induced crystallization of a Nb nanowire. (a) As-produced 5 nm wide Nb wire before intense irradiation. The wire was prepared by sputtering a 3 nm layer of Nb on a suspended nanotube. Unlike in figure 2 showing granular AuPd wire, no such granularity was observed on this amorphous Nb wire. (b) The same wire after being exposed to a dose of electrons of ∼700 pC nm^{-2}. The irradiation was performed under low current density, to avoid excessive sample heating (the intensity of ∼0.4 pA nm^{-2} was sustained for 30 min).

3. Results and discussion

It is known from the literature that thin sputter-deposited films of MoGe are amorphous and continuous [11], while Nb films can have a nanocrystalline structure [12]. Our TEM imaging, on the other hand, showed that nanotube-templated MoGe and thin enough Nb wires are amorphous (figures 3(a) and 4(a)). Thicker Nb wires remained continuous but showed nanocrystalline structure for diameters larger than ∼10 nm.

An important observation, which can be used in the fabrication of nanodevices, is the possibility of modifying the crystal structure of nanowires under the influence of high energy electron radiation. We observed that amorphous wires of various diameters (∼4–10 nm) became crystalline after a long enough irradiation with the TEM beam. This effect is illustrated in figure 3, where a Nb nanowire is shown before (a) and after (b) the irradiation with a 200 keV electron beam. The irradiation was done by continuous imaging (using the same beam strength as was used for normal TEM imaging) during a time interval of approximately 30 min. Note that some signatures of crystallization were already observed after 5 min of imaging. Irradiation of MoGe nanowires under similar conditions was also carried out; see figure 4. This figure shows that MoGe can be crystallized as effectively as Nb. An approximate minimum dose of electrons required to observe any crystallization in Nb or MoGe wires was 50 pC nm^{-2}. Tests with different beam intensities (current densities ranging from 0.3 to 30 pA nm^{-2}) showed that only the rate of crystallization depended on the intensity of the beam. Crystallization occurred at any intensity from the test interval 0.3–30 pA nm^{-2}. One way to understand this effect is by assuming that the thermal heating effects are not very

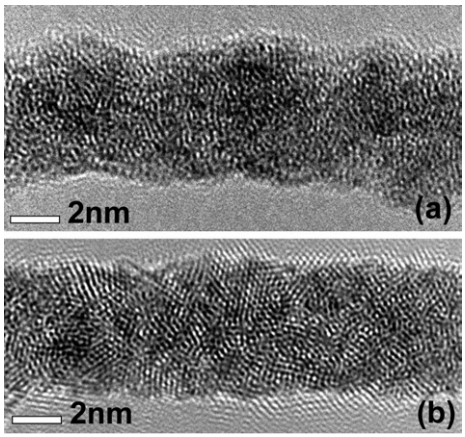

Figure 4. Electron-beam induced crystallization of a MoGe wire. (a) A high resolution image of as-grown 5.5 nm wide MoGe. No granularity is observed on MoGe samples before e-beam exposure. The homogeneity of MoGe wires is related to their amorphous structure. (b) The same wire after being subjected to an electron dose of ∼900 pC nm^{-2}.

significant. Other explanations may also be possible and further investigation is required in order to establish this.

Electron-beam induced crystallization, such as that described above, has been studied previously on larger samples made of different materials: Si [13, 14], Ge [13], GaAs [13] GeAu [15] etc. We believe that the mechanism of crystallization described in these previous studies is also valid for the crystallization of our samples. Most importantly, the crystallization is not induced by heating the wire, but by displacement of atoms in electron–atom collisions. The energy threshold required to displace atoms depends on the atomic mass of the material and the bond strength. This displacement threshold, E_D, is the kinetic energy an atom needs to possess in order to be displaced. Approximate displacement threshold values for the elements used are $E_D = 24$ eV (for Nb) [16], $E_D = 27$ eV (for Mo) [16] and $E_D = 20$ eV (for Ge) [17]. Since electrons colliding with atoms cannot transfer all their energy into the kinetic energy of the crystal atoms, they have to be accelerated to a much higher energies than the displacement threshold. The electronic energies required to initiate crystallization (E_t) are given by the Hobbs formula

$$E_t = 0.05[(0.2(100 + AE_D))^{1/2} - 10],$$

obtained from [18], where A is the atomic weight. We calculate the energies required to crystallize the sample as $E_t = 579$, 659 and 380 keV. Although the accelerating voltage of our TEM is 200 keV, it is still possible that electron–atom collisions play a key role in the observed crystallization (and also induce etching as discussed below). The reason for such a conclusion is that multiple previous studies [13, 14] indicated that crystallization could be induced by electron irradiation with sub-threshold energies. Therefore, we conclude that the observed crystallization of nanowires was induced by electron–atom collisions, and not by sample heating. This conclusion is also supported by the following two observations: (i) crystallization occurred at any beam current density and (ii) complete crystallization occurred at similar electron doses for samples with different geometrical characteristics.

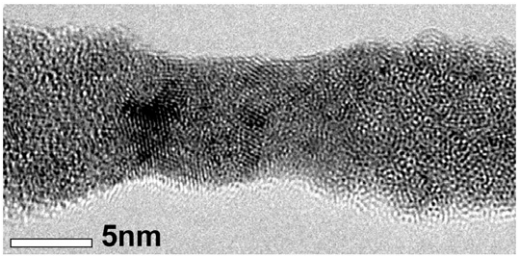

Figure 5. Selective crystallization of an amorphous Nb nanowire. The ends of the wire have been exposed to a very low dose of e-beam radiation, which is just sufficient to take the picture. The ∼11 nm long segment in the centre of the wire received an e-beam dose of ∼530 pC nm^{-1} (9 pA nm^{-2} over 60 s). The micrograph was obtained at a current density ten times lower that the one used to crystallize the centre of the wire. Therefore the imaging did not cause significant crystallization.

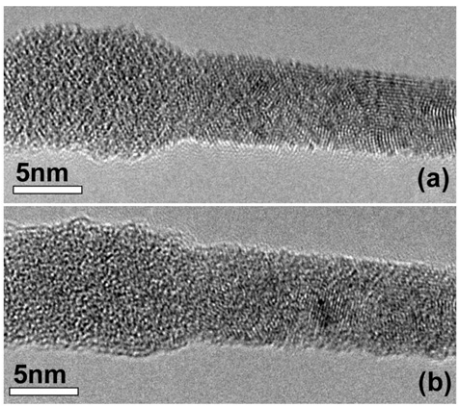

Figure 6. (a) Electron-beam induced crystallization and etching of a Nb nanowire. The initial diameter of the nanowire was ∼9 nm. The right-hand side of the wire was selectively exposed to electron-beam radiation. The right-hand side is crystallized and reduced in diameter (new diameter is ∼6 nm), while the left-hand side is unchanged and remains amorphous. (b) The same wire after exposure to air at room temperature for 1 h. Some oxidation (∼1–2 nm) is evident on the surface. However, the characteristic pattern of fringes, representing nanocrystals, is still present at the core of the wire.

We also successfully achieved spatially localized crystallization, i.e. a crystallization of a short segment of the wire. Good focus of the TEM beam allowed a small segment of the wire to be irradiated. Hence, sections of a wire could be selectively crystallized, leaving the rest of the wire amorphous. In such experiments the electron current density was kept at a value below 10 pA nm^{-2} in order to avoid excessive heating and e-beam etching (see below) of the wire. Figure 5 shows an example of an amorphous wire with an ∼11 nm segment that has been crystallized by a TEM beam. This result can be used for the fabrication of sub-10 nm patterns *within a single nanowire*.

Another effect that occurs along with crystallization is etching or sputtering of the wire, induced by e-beam irradiation. Sputtering of the metal from the nanowire is expected for electron energies above 50% of the displacement threshold [19]. This effect is expected to occur at any beam current density, because it depends only on the energy of incident electrons. In our experiments crystallization occurred much more rapidly than sputtering of the material. Therefore, using a minimum electron dose and low current density (below 10 pA nm^{-2}) provided us with enough control to be able to crystallize samples without causing noticeable material loss.

Figure 6 shows a nanowire before and after an exposure to a focused electron beam for 60 s, with the current density of ∼20 pA nm^{-2}. In this test the electron beam was focused in such way that only the right-hand side of the wire was exposed to intense e-beam radiation. We find that the right-hand side of the wire was not only crystallized but also reduced in diameter. The width of the transition region between the unexposed left-hand side (which remains amorphous) and the exposed right-hand side (which is crystallized and reduced in diameter by the e-beam etching) is about 3 nm. Such processing could potentially be used to manufacture wires of very specific diameters, significantly smaller than 10 nm. It is also important that a direct visual control is provided in the TEM, so the etching process can be stopped as soon as the desired shape of the wire is achieved.

In order to test the stability of thus-obtained wires, this wire was removed from the TEM, after the completion of the crystallization, and exposed to air at room temperature for 1 h. Subsequent imaging of the wire (figure 6(b)) showed that some oxidation occurred; however the crystalline pattern in the core of the wire was mostly unaffected (figure 6(b)). Thus the wires show a promising stability for room temperature nanodevices. Note that the local e-beam etching described here can be exploited as a powerful method allowing modification and local tuning of the wire diameter at a scale and with a resolution of just a few nanometres, under direct visual control.

The capability to locally change the diameter of the wire can be applied for fabrication of local barriers, which can be used to limit the propagation of electrons along the wire and, if sufficiently strong, to localize the electronic wavefunction between a pair of barriers. A structure with two e-beam etched barriers is shown in figure 7. Such a system can function as a single-electron transistor (SET). Experimentally, such transistors have been extensively studied [2]. The new result that we report is the fabrication method that gives extremely small devices with high charging energies and consequently high expected operation temperatures. For a discussion of the principles of SET operation see [20].

A qualitatively different phenomenon was observed at even higher irradiation current densities (20–30 pA nm^{-2}). At such conditions the material of the wire was not only sputtered away and crystallized, but also formed well-defined nanometre-size grains at the points of greatest intensity of the beam (figure 8). Visual observation of the process suggests that local melting occurs in such cases. The phenomenon is more pronounced in wires with smaller diameters, supporting our assumption about overheating and possible local melting of the wire. In figure 8 we present an example of a nanograin formed at the constriction that was created by a high intensity strongly focused electron beam. If the resistance between the grain and the wire is high enough, the resulting device can act as an SET transistor. Such focused e-beam melting gives the smallest grain size in the range ∼3.5 nm. The charging energy for such nanograins can be estimated as 0.5 eV or 6000 K, much higher than the room temperature. Thus such single-electron tunnelling devices could show a transistor effect even at room temperature. Observation of discreteness of the electronic

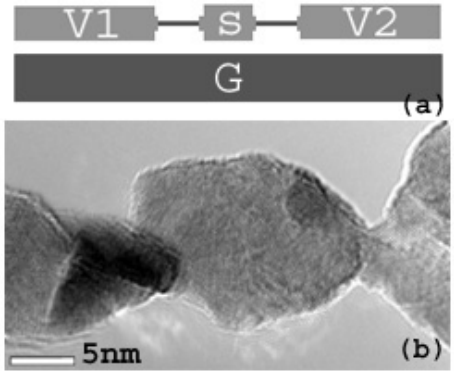

Figure 7. An example of a structure that can possibly function as a single-electron tunnelling (SET) device. The structure is created within a Nb nanowire using electron-beam etching. (a) A schematic diagram of an SET transistor. V1, V2 are the source and drain electrodes respectively. The Coulomb island is marked 'S' and represents the central metallic grain with a localized electronic cloud. The localization is achieved due to barriers shown schematically as solid lines. The gate electrode, marked 'G', can be used for tuning the electric potential of the Coulomb island, thus controlling the electrical current through the Coulomb island. (b) A micrograph of an e-beam produced structure that can possibly function as an SET device is shown. Two constrictions were created in an 15 nm Nb wire, and positioned approximately 20 nm apart. The gate is not present.

spectrum could also be achieved with such samples. We intend to perform transport measurements on such devices in the near future.

4. Conclusions

We prepared suspended metallic nanowires with sub-10 nm diameters and observed four related but distinct processes caused by the electron-beam irradiation: (1) crystallization of initially amorphous nanowires; (2) local crystallization induced by a focused electron beam; (3) local etching (or sputtering) of the wire observed after a longer exposure to the e-beam; (4) possible melting and formation of a single nanograin in the wire, caused by a highly focused e-beam of high intensity. Crystallization is expected to be caused by knock-on atom displacements. Loss of material (etching) was observed at any intensity of the beam; however, it only became significant at electron doses up to 2–3 times greater than those required to cause complete crystallization. Formation of grains was observed at the highest beam intensities (current density above 20 pA nm^{-2}) and also appeared to be more prevalent in thin wires ($\sim$3 nm). This suggests that the formation of grains is caused by local heating of the wire; hence it only occurs when heat transferred from the e-beam is not conducted away too rapidly and is sufficient for the melting to occur.

The effects described can be used for nanometre scale modification of the structure and geometry of nanowires at a scale significantly smaller than 10 nm. The method opens a large number of possibilities for the fabrication of metallic nanodevices at this small scale. In particular we suggest that ultrasmall single-electron tunnelling transistors operational at room temperature can be produced using the approach outlined. Fabrication and testing of such transistors is our goal for the future.

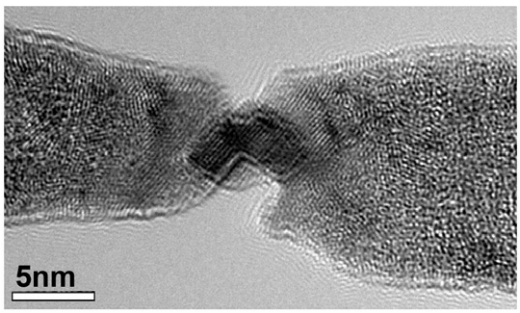

Figure 8. Electron-beam sculpting of a constriction with a $\sim$3.5 nm wide grain. The nanograin is created in a Nb wire by a focused electron beam, which can possibly melt the material locally. The middle segment has been subjected to irradiation, while the ends are still amorphous, confirming that the electron beam was well focused. The structure can possibly function as a room temperature single-electron device.

Acknowledgments

The authors thank M Murphey and J Hughes for their help with the sample preparation, and J Wen and R Twesten for technical advice regarding TEM operation. The work was supported by NSF CAREER Grant No. DMR 01-34770, by the Alfred P Sloan Foundation and by a DOE grant DEFG02-91-ER45439. Part of the work was carried out in the Center for Microanalysis of Materials, University of Illinois, which is partially supported by the US Department of Energy under grant DEFG02-91-ER45439.

References

[1] Cumming D R S *et al* 1995 *Appl. Phys. Lett.* **68** 322
[2] Fulton T A and Dolan G J 1987 *Phys. Rev. Lett.* **59** 109
[3] Grabert H and Devoret M H (ed) 1992 *Single Charge Tunneling: Coulomb Blockade Phenomena in Nanostructures* (*NATO ASI Series. Series B, Physics* vol 294) (New York: Plenum)
[4] Bezryadin A, Lau C N and Tinkham M 2000 *Nature* **404** 971
[5] Bezryadin A and Dekker C 1997 *J. Vac. Sci. Technol.* B **15** 793
[6] Zhang Y and Dai H 2000 *Appl. Phys. Lett.* **77** 3015
[7] Hopkins D, Pekker D, Goldbart P M and Bezryadin A 2005 in preparation
[8] Braun E, Eichen Y, Sivan U and Ben-Yosef G 1998 *Nature* **391** 775
[9] Richter J *et al* 2001 *Appl. Phys. Lett.* **78** 536
[10] Rogachev A and Bezryadin A 2003 *Appl. Phys. Lett.* **83** 512
[11] Graybeal J M *et al* 1987 *Phys. Rev. Lett.* **59** 2697
[12] Mayadas A F, Laibowitz R B and Cuomo J J 1972 *J. Appl. Phys.* **43** 1287
[13] Jenčič I, Bench M W, Robertson I M and Kirk M A 1995 *J. Appl. Phys.* **78** 974
[14] Lulli G, Merli P G and Antisari M V 1987 *Phys. Rev.* B **36** 8038
[15] Long B, Yong Q and Ziqin W 1996 *J. Appl. Phys.* **80** 6170
[16] Phillipp F, Saile B, Schmid M and Urban K 1979 *Phys. Lett.* A **73** 123
[17] Mooney P M and Bourgoin J C 1984 *Phys. Rev.* B **29** 1962
[18] Williams D B and Carter C B 1996 *Transmission Electron Microscopy* vol 1 (New York: Plenum) p 63
[19] Williams D B and Carter C B 1996 *Transmission Electron Microscopy* vol 1 (New York: Plenum) p 65
[20] Kastner M A 1993 *Phys. Today* **46** (1) 24